Role of Surface Enhancement in the Enzymatic Cross-Linking of Lignosulfonate Using Alternative Downstream Techniques

Sidhant Satya Prakash Padhi,* Miguel Jimenez Bartolome, Gibson Stephen Nyanhongo, Nikolaus Schwaiger, Alessandro Pellis, Hendrikus W. G. van Herwijnen, and Georg M. Guebitz

Read Online

ACCESS | Metrics & More | Article Recommendations | Supporting Information

ABSTRACT: Lignosulfonate (LS), one of the byproducts of the paper and pulp industry, was mainly used as an energy source in the last decade until the valorization of lignin through different functionalization methods grew in importance. Polymerization using multicopper oxidase laccase (from the *Myceliophthora thermophila* fungus) is one of such methods, which not only enhances properties such as hydrophobicity, flame retardancy, and bonding properties but can also be used for food and possesses pharmaceutical-like antimicrobial properties and aesthetic features of materials. Appropriate downstream processing methods are needed to produce solids that allow the preservation of particle morphology, a vital factor for the valorization process. In this work, an optimization of the enzymatic polymerization via spray-drying of LS was investigated. The response surface methodology was used to optimize the drying process, reduce the polymerization time, and maximize the dried mass yield. Particles formed showed a concave morphology and enhanced solubility while the temperature sensitivity of spray-drying protected the phenol functionalities beneficial for polymerization. Using the optimized parameters, a yield of 65% in a polymerization time of only 13 min was obtained. The experimental values were found to be in agreement with the predicted values of the factors (R^2: 95.2% and p-value: 0.0001), indicating the suitability of the model in predicting polymerization time and yield of the spray-drying process.
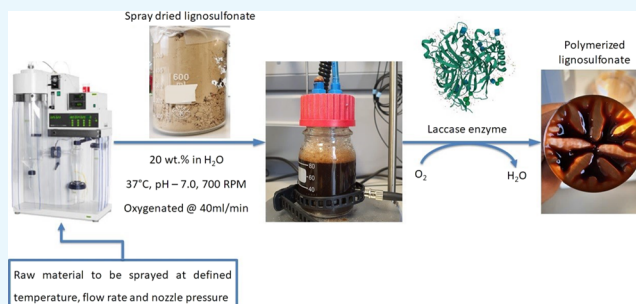
1. INTRODUCTION

Biomass valorization is an ongoing challenge for the forest-based industry, which consists of three main components: cellulose, hemicellulose, and lignin. Lignin is the largest source of natural aromatic compounds such as p-coumaryl, coniferyl, and sinapyl alcohols, yet only 1−2% of the total lignin produced is valorized to produce composites, tanning pigments, polymer blends, and thermosetting adhesives, which shows the potential along with the underutilization of this biopolymer.[1] Lignosulfonates (LSs) are a common byproduct produced after the sulfite pulping process, resulting as a black liquor. In the modern era, integrated biorefineries are introduced as a method to increase the economic viability of the pulping industry.[2] There is a wide variety of approaches to tailor lignin properties for specific applications, including the use of high energy demanding physical processes, composites, fillers, alloys, pharmaceutical applications through blending, chemical, and enzymatic processes.[3−5] Polymerization of technical lignosulfonate is one such process using a laccase-catalyzed oxidation process that attacks the phenolic hydroxyl groups of the material, resulting in the generation of reactive species such as phenoxy radicals, peroxy radicals, semi-quinones, and quinones.[3,6,7] All these reactive species react among themselves or with other molecules present in the

reaction environment, leading to the formation of several kinds of interunit linkages, including but not limited to β-O-4′, β-5′, 5−5′, β-β′, and 5-O-4′, and forming a series of aromatic polymers having different sizes and complexities.[8]

Soluble LS should be dried out for a better storage, as well as processability of the material. However, the impact of drying onto enzymatic polymerization has not yet been studied to the best of our knowledge. Spray-drying is the most economical method in maintaining high-quality products by rapid dehydration. It provides a large surface area in the form of fine liquid droplets through atomization in the drying chamber, which leads to the production of regularly and spherically shaped powder particles.[4] The literature shows that physical properties of the powdered product, that is, the moisture content, the bulk density, and the particle size are significantly affected by the drying temperature and the carrier agent.[4,9,10] Nevertheless, to produce a material with the required
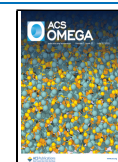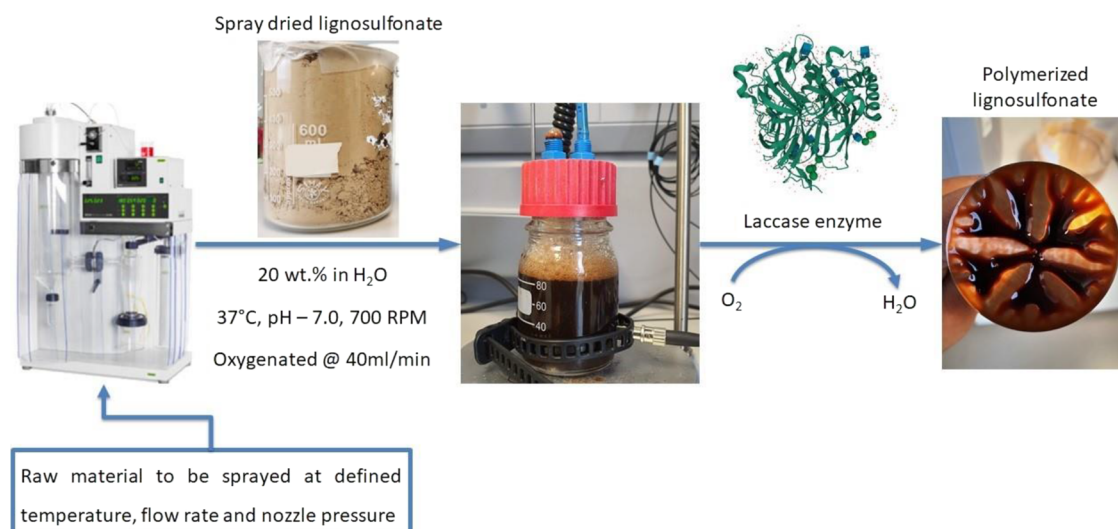
Figure 1. Schematic diagram summarizing the developed process.

Table 1. Optimization of Spray-Drying for the Enzymatic Polymerization of LS: Coded Factors of the Design of Experiment

factor	name	min	max	coded low	coded high	mean	std. dev.
A	temperature [°C]	136.4	203.6	−1 ↔ 150.0	+1 ↔ 190.0	170.0	16.96
B	feeding rate [%]	23.2	56.8	−1 ↔ 30.0	+1 ↔ 50.0	40.0	8.48
C	nozzle pressure [%]	23	57	−1 ↔ 30.0	+1 ↔ 50.0	40.0	8.48

properties, it is necessary to find appropriate parameters for drying a material using such a technique. In this study, spray-drying process parameters were used as a mean to obtain optimal results, considering parameters such as the moisture content or the amount of dried materials obtained and the polymerization time (Figure 1).

2. MATERIALS AND METHODS

2.1. Chemicals. All used chemicals and solvents used were of analytical grade. Sodium hydroxide (NaOH) and sodium azide (NaN_3) were obtained from Carl Roth (Karlsruhe, Germany); sodium acetate ($CH_3COONa \cdot 3H_2O$), sodium carbonate (Na_2CO_3), vanillin, and Folin−Ciocalteu reagent were obtained from Sigma Aldrich (Karlsruhe, Germany); the zeta potential standard was supplied by Malvern Panalytical (Wolkersdorf, Austria); sodium nitrate ($NaNO_3$) from Merck (Darmstadt, Germany); the bovine serum albumin (BSA) standard was obtained from BioRAD (Vienna, Austria); MtL (*Myceliophthora thermophila* laccase) from Novozymes (Novozym 51003) and industrial-grade Mg-lignosulfonate with an average M_w of 30 ± 5 kDa was provided by SAPPI GmbH (Gratkorn, Austria).

2.2. Design of Experiment. A three factorial central composite rotatable design (CCRD) was used. A quadratic and reduced quartic model between the factors (process variables) and the polymerization time as well as the yield of the dried mass was estimated. The factors studied were the drying temperature (A: 150−170 °C), feeding rate (C: 30−40% of the maximum possible feeding rate), and the nozzle pressure (B: 30−40 mL/min), while the response variables were the dried mass (Y_1), which was the exclusion of the water content in the powder and the time needed for polymerization to reach a viscosity of 300 mPa s (Y_2). Each factor was coded as low (−1), high (+1), and mean (0) shown in Table 1. Twenty randomized trials were carried out including the six central

replicates that were assigned based on the structure of the design model (found in Table ST1 in the Supporting Information). The experimental conditions that were identified as the optimum for the required time of polymerization was performed six times.

The estimated quadratic model was considered, and its coefficients were evaluated. ANOVA analysis was used to establish the significance of the response (Y_1: dried mass content). The second response (Y_2: time needed for polymerization to reach a viscosity of 300 mPa s) was fitted using a reduced quartic model along with the analysis of variance (ANOVA). Finally, an optimization procedure was used for the adjusted model to find the optimal conditions. The two applied models to predict the responses are mentioned below in eqs 1 and 2:

Equation 1 Quadratic model

$$Y_1 = b_0 + b_1A + b_2B + b_3C + b_{12}AB + b_{13}AC + b_{23}BC + b_{11}A^2 + b_{22}B^2 + b_3C^2 \tag{1}$$

Equation 2 Reduced Quartic model

$$Y_2 = b_0 + b_1A + b_2B + b_3C + b_{12}AB + b_{13}AC + b_{23}BC + b_{123}ABC + c_{12}A^2B + c_{23}B^2C + d_{12}A^2B^2 \tag{2}$$

2.3. Spray-Drying. A volume of 1200 mL (17% solid content) was taken in each run for the spray-drying of the samples. The different operation parameters (i.e., temperature, feeding rate, and flow rate for atomization) were selected on the BUCHI mini Spray Dryer B-290. The fine dried fraction was collected and measured for mass and moisture content to calculate the total dried mass obtained in each run. Said samples were then used in the enzymatic polymerization process at a solid concentration of 20 wt %. As control, the process was compared with classical oven-dried LS.

Table 2. ANOVA of the Yield of Dried Mass (Y_1)

source	sum of squares	df	mean square	F-value	p-value	
model	15615.16	9	1735.02	11.37	0.0004	**significant**
A-temperature	2483.43	1	2483.43	16.28	0.0024	
B-feeding rate	5372.65	1	5372.65	35.21	0.0001	
C-nozzle pressure	603.21	1	603.21	3.95	0.0748	
AB	300.13	1	300.13	1.97	0.1910	
AC	2.42	1	2.42	0.0159	0.9023	
BC	4.20	1	4.20	0.0276	0.8715	
A^2	16.51	1	16.51	0.1082	0.7490	
B^2	233.19	1	233.19	1.53	0.2446	
C^2	6775.25	1	6775.25	44.41	<0.0001	
residual	1525.69	10	152.57			
lack of fit	1178.91	5	235.78	3.40	0.1027	**not significant**
pure error	346.78	5	69.36			
cor total	17140.85	19				
R^2	0.9110					

2.4. Polymerization. Each of the dried LS samples was resuspended in ultrapure water at 20 wt % and left for stirring at 40 °C until completely solubilized, followed with a NaOH addition to reach pH 7 (pH at which MtL shows the highest catalytic activity).[11] Enzymatic oxidation was carried out in 500 mL transparent durum bottles with tight-fitting tube holes on the lid to allow the air supply. The reaction was started by introducing 233 nkat/mL laccase and was continuously supplied with 10 cm^3/min oxygen at 37.5 °C while mixing under vigorous stirring at 900 rpm. The reaction was stopped when the material turned into a solid gel (>1000 mPa s) or at 20 min, taking samples for measurement each 5 min.

2.5. Viscosity. Realtime measurement of the viscosity was carried out using an Anton Paar rheometer (MCR 302) to observe the growth of the polymer matrix chain in the system by taking samples of 0.7 mL (0.653 mL advised by Anton Paar) every 5 min. The samples were measured under a constant shear rate of 200/s for a period of 10 s at 20 °C using a 50 mm cone plate setup. The average value of the viscosity in mPa s was evaluated by the instrument using a predefined protocol setup by the user.

2.6. Thermo-Analytical Analysis. A thermogravimetric analyzer (Netzsch TG 209 F1) was used to carry out the decomposition analysis of unpolymerized and polymerized lignin from ambient temperature to 900 °C at a heating rate of 10 °C/min under an ambient atmosphere with a flow rate of 20 mL/min.

2.7. Zeta Potential and Size Characterization. Samples were measured at 25 °C on a Zetasizer Nano ZS fitted with a folded capillary zeta cell (DTS1070). Unpolymerized lignin and polymerized lignin were measured in 1 mM NaOH. The concentration of the samples was prepared in 1% v/v in ultrapure water at pH of 7 ± 0.02 to maintain ionic strength and to ensure that the differences in the measured electrophoretic mobilities are not due to variation in conductivity.

For all measurements, auto selection of voltage was chosen with measurement gaps of 2 mm. Six repetitions of each sample were made, and the measured electrophoretic mobilities were converted into zeta potential using the Smoluchowski's formula.

Size characterization of the samples was made by dynamic light scattering (DLS) measurements using the Zetasizer Nano ZS at a selected wavelength of 633 nm and a detection angle of 173 °C. The intensity is averaged particle diameters, and the

dispersity index (Đ) values are also calculated from the cumulants analysis defined in ISO 13321.

2.8. Scanning Electron Microscopy Analysis. In order to determine possible morphological differences in the LS obtained with the drying methods (oven-dried and spray-dried), scanning electron microscopy (SEM) analysis was carried out. Images with 2500 and 6000 augments were taken using a Hitachi Table-top Microscope TM3030 at both 15 kV and EDX methods of accelerating voltages and at 182.65 DPI. Multiple magnifications were used such as ×100, ×500, ×1000, and ×1200.

2.9. Size Exclusion Chromatography Analysis. As described previously,[12] size exclusion chromatography (SEC) was used to monitor molecular weight changes during laccase-mediated polymerization of LS. Samples with a volume of 0.5 mL were withdrawn from the lignin material and diluted with the mobile phase (50 mM NaNO$_3$, 3 mM NaN$_3$) to a concentration of 1 mg mL^{-1} before injecting 100 μL into the system. The SEC system was equipped with a quaternary/binary pump, an auto sampler 1260 series from Agilent Technologies (Palo Alto, CA), DAD- (diode array detector), an RI (Refractive Index)-detector system (Agilent Technologies 1260 Infinity), and a MALLS HELEOS DAWN II detector from Wyatt Technologies (Dernbach, Germany). The separation was carried out using a precolumn PL aquagel-OH MIXED Guard (PL1149−1840, 8-μm, 7.5 × 50 mm, Agilent, Palo Alto, CA) and a separation column PL aquagel-OH MIXED H (PL1549−5800, 4.6 × 250 mm, 8 μm, Agilent, Palo Alto, CA) with a mass range from 6 to 10,000 kDa. BSA was used as the standard for normalization, band broadening, and alignment of the MALLS detector. The Agilent Software Openlab Chemstation CDS, as well the ASTRA 7 software from Wyatt Technologies, were used for data acquisition and data analysis.

2.10. Phenolic Content. Variances in the number of phenolic groups between the different dried LS samples obtained were determined using the Folin−Ciocalteu (FC) assay described in a previous study.[13] Diluted LS samples (0.8 g/L) were mixed with the FC reagent, vortexed, and then incubated at 21 °C for 5−8 min. After that, an incubation in a 20% Na$_2$CO$_3$ solution for 2 h at 21 °C and 800 rpm was performed. The samples were then plated in a 96-well plate, and the absorbance was measured at 760 nm in a TECAN

Table 3. ANOVA of the Polymerization Time (Y_2)

source	sum of squares	df	mean square	F-value	p-value	
model	366.42	10	36.64	17.80	<0.0001	**significant**
A-temperature	38.89	1	38.89	18.89	0.0019	
B-feeding rate	2.00	1	2.00	0.9715	0.3501	
C-nozzle pressure	2.00	1	2.00	0.9715	0.3501	
AB	50.00	1	50.00	24.29	0.0008	
AC	40.50	1	40.50	19.67	0.0016	
BC	50.00	1	50.00	24.29	0.0008	
ABC	50.00	1	50.00	24.29	0.0008	
A^2B	12.03	1	12.03	5.84	0.0388	
B^2C	15.39	1	15.39	7.48	0.0231	
A^2B^2	22.53	1	22.53	10.95	0.0091	
residual	18.53	9	2.06			
lack of fit	13.20	4	3.30	3.09	0.1236	**not significant**
pure error	5.33	5	1.07			
cor total	384.95	19				
R^2	0.9519					

plate reader (Infinite M200, Switzerland) and compared with a vanillin solution as a standard.

3. RESULTS AND DISCUSSION

The three factors that affect the yield and morphology of the particles are atomization pressure, feeding rate, and temperature. Each of the factors combined together has a multivariate contribution to the overall formation of particles. These effects that lead to particle formation were later analyzed on the enhancement of the polymerization of LS in terms of the zeta potential, TGA, and SEC analysis.

3.1. Design of Experiments. The literature has shown that the properties of powders obtained by spray-drying mainly depend on the operational characteristics like the feeding rate, drying gas temperature, and atomization pressure. The goal of the work was to evaluate to what extent each of these factors affects the polymerization time of the LS and compare it to the other drying methods, that is, traditional oven-drying. Through the design of experiments, 20 randomized runs were sprayed for the given conditions, and from that, the mass of the dried material in the fines were collected and was measured against the fixed volume sprayed in each case (1200 mL with 17% solid content). The dried powder was then used in the enzymatic polymerization process, and the design model was further investigated.

3.1.1. Yield of Dried Mass. The ANOVA analysis for the polynomial equation for each response can be observed in the Table 2 where it is shown that the model was significant with a *p*-value of 0.0004 (mostly affected by the linear terms and quadratic terms). The model was optimized at confidence intervals of 95%, and the data can be seen in eq 3; the model graphs can be found in Figure S1 of the Supporting Information.

Yield of Dried Mass (Y_1)

$$= -251.81 + 0.469 \times \text{temperature}$$
$$- 3.682 \times \text{feeding rate} + 18.768 \times \text{nozzle pressure}$$
$$+ 0.031 \times \text{temperature} \times \text{ feeding rate}$$
$$- 0.003 \times \text{temperature} \times \text{nozzle pressure}$$
$$- 0.007 \times \text{feeding rate} \times \text{nozzle pressure}$$
$$- 0.003 \times \text{temperature}^2 - 0.040 \times \text{feeding rate}^2$$
$$- 0.217 \times \text{nozzle pressure}^{22} \tag{3}$$

3.1.2. Enzymatic Polymerization Time. The ANOVA of the enzymatic polymerization time is more complex because of the involvement of the enzymes due to which a reduced quartic model was chosen (significance with a *p*-value of <0.0001 with linear, quadratic, cubic, and quartic terms seen to be significant in Table 3). The R^2 of the model was also found to be 0.9519; the regression coefficients can be seen in eq 4 below, and model graphs can be found in Figure S2 of the Supporting Information.

Polymerisation time (Y_2)

$$= 322.46 - 2.184 \times \text{temperature} - 9.295$$
$$\times \text{feeding rate} - 5.091 \times \text{nozzle pressure}$$
$$+ 0.062 \times \text{temperature} \times \text{feeding rate}$$
$$+ 0.039 \times \text{temperature} \times \text{nozzle pressure}$$
$$+ 0.118 \times \text{feeding rate} \times \text{nozzle pressure}$$
$$- 0.001 \times \text{temperature} \times \text{feeding rate}$$
$$\times \text{nozzle pressure} + 0.001 \times \text{temperature}^2$$
$$\times \text{feeding rate} + 0.002 \times \text{feeding rate}^2$$
$$\times \text{nozzle pressure} - 2 \times 10^{-6} \times \text{temperature}^2$$
$$\times \text{feeding rate}^2 \tag{4}$$

The nonsignificant residuals for both the responses yield of dried mass and polymerization time had a *p*-value of 0.1027 and 0.1236, respectively, along with an *F*-value of the model to

be 11.37 and 17.80, respectively, showed that the fitting of the model was appropriate. The probability of occurring noise for the responses is 0.04 and 0.01%. Most of the nonsignificant *p*-values of the model parameters were removed to attain a better fitting of the model.

3.2. Regression of the Enzymatic Polymerization.
The progress of polymerization was described based on the fitting data of the polymerization with respect to time and viscosity change during polymerization. The model followed an exponential increase in the viscosity with respect to time with eq 5 being

$$\text{viscosity} = b_0 e^{b_1(\text{time})} \tag{5}$$

where b_1 is the viscosity time factor $[\text{s}^{-1}]$ and b_0 is the initial viscosity $[\text{mPa s}]$.

The exponential regression of the viscosity change showed the equation to fit with a R^2 of more than 90% for all the runs. Based on the data observed from the equation, the time required for the viscosity to reach 300 mPa s was calculated in each case, and the optimized run was compared to the equation as well as the modeling of the DoE. The R^2 value of the optimized regression was 97.9% with an experimental deviation of 8.33% from the predicted values with eq 6 being

$$\text{viscosity (mPa s)} = 3.291 e^{0.3473(\text{time (s)})} \tag{6}$$

3.3. Solubility.
Spray-dried LS solubility was correlated to the change in viscosity of the material, as shown in Figure 2.
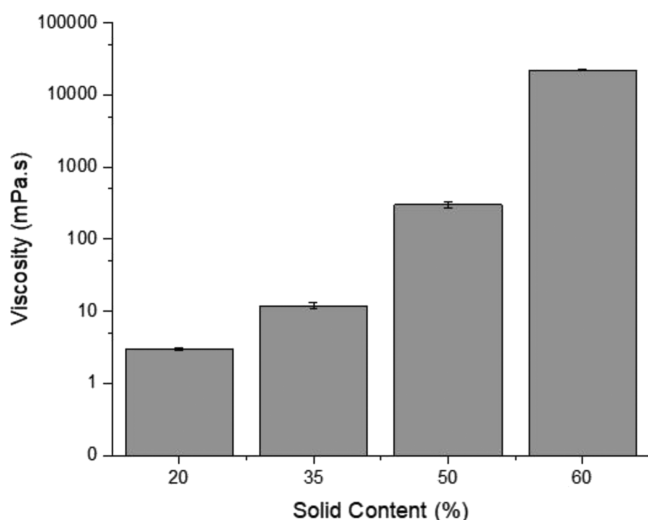

Figure 2. Effect of the solid content on the viscosity of the spray-dried LS.

The increase in viscosity was exponential with linear change in the solid content. At 20% solid content, the viscosity of the material was 3 mPa s at 200/s of shear rate in a cone plate setup, whereas the viscosity of the solution went up to 22,000 mPa s at 60% solid content. It can be observed that with a 40% increase in the solid content, the viscosity change was in the factor of 7300. In the case of the spray-dried LS, the particle sizes were significantly smaller (385 nm) and had a significantly lower surface area, thus enhancing the initial wetting of the sample. In case of amorphous solids such as lignin, lattice energy plays a minor role in solubility, but the effect of the surface area and the particle size has direct proportionality in the solubility of a powder in the solvent

medium. Two phenomena that dominate the solubility of a particle are surface wetting and the diffusion of the solvent into the pores of the solids.[14] Literature studies on contact angle measurements of the LS indicated that the amorphous behavior negates the lattice energy limitations seen in crystals while the smaller size of particles had higher wetting and faster diffusion of water into the solid.[15]

3.4. Particle Morphology.
The morphological characterization of the dried LS powders was conducted via SEM. The particles were obtained using both oven-drying and spray-drying (Figure 3) processes, the depicted particles were from the optimized run of the spray-drying carried out at a temperature of 190 °C, a feeding rate of 38% (12 mL/min), and an atomization rate of 46 mL/min. The most prominent morphology within the two different kinds of the drying methods is the rough irregular shaped larger particles that can be seen in oven-dried as compared to the globular, double concave-shaped spray-dried LS. Other authors have reported that the surface roughness of the particles increase with the increase in the outlet temperature of the system, such as seen in the case of microcrystalline cellulose and mannitol.[4,16] The smooth spherical surfaces were found with the outlet temperature being up to 65 °C, and the rough particle surfaces were found in the range of 120 to 150°C.[17] In this work, the outlet temperature varied between 40 and 45 °C.

A smooth double concave hollow structure is seen in the case of the spray-dried LS with a smaller particle size distribution as compared to the oven-dried LS. It produces particles with higher porosity and more surface area for surface wetting and increase in solubility, which in turn enhances the enzyme action during polymerization.[4,18] In the case of enzymes, the surface topography plays a major role in activity. In studies, it had been observed that the regularity of the surface allows the prolonged retention of enzyme activity.[19] Similar effects were also seen with lactase with lower surface roughness of PMMA directly affecting the increase retention of lactase activity.[18−20]

3.5. Cross-Linking.
Incubation of laccase with the LS while continuously adding oxygen steadily increased their molecular weight from an average 28 to >359 kDa in 16 min for the spray-dried samples and from an average of 39 to >325 kDa in 16 min for the oven-dried samples. The increase in molecular weight was also accompanied by a continuous increase in viscosity. The viscosity of unpolymerized lignin, with an average of 5.3 mPa s, increased to more than 3000 mPa s (5232 mPa s for spray-dried and 3560 mPa s for oven-dried) after 20 min of polymerization. The particle morphology and solubility explain the increase in cross-linking thorough polymerization. The combined effects of particle properties such as the surface charge and size (Section 3.8) and topography and roughness (Section 3.4) on the process of polymerization have been discussed in detail. With the spray-drying method modification of the substrate from oven-drying to spray-drying, the polymerization rate has enhanced from 328 to 414 Da/s. Moreover, higher-molecular-weight polymers are formed from spray-dried lignin when compared to oven-dried lignin most likely due to the preservation of the phenolic content,[21,22] as can be seen in Figure 4.

The increase in the viscoelastic behavior of lignin with the ongoing polymerization is due to the increase in the molecular weight of the material, thanks to the cross-linking formed by the laccase enzyme.[6,23] At the beginning of the polymerization, the viscosity can be called as zero-time viscosity (5.3 mPa s at
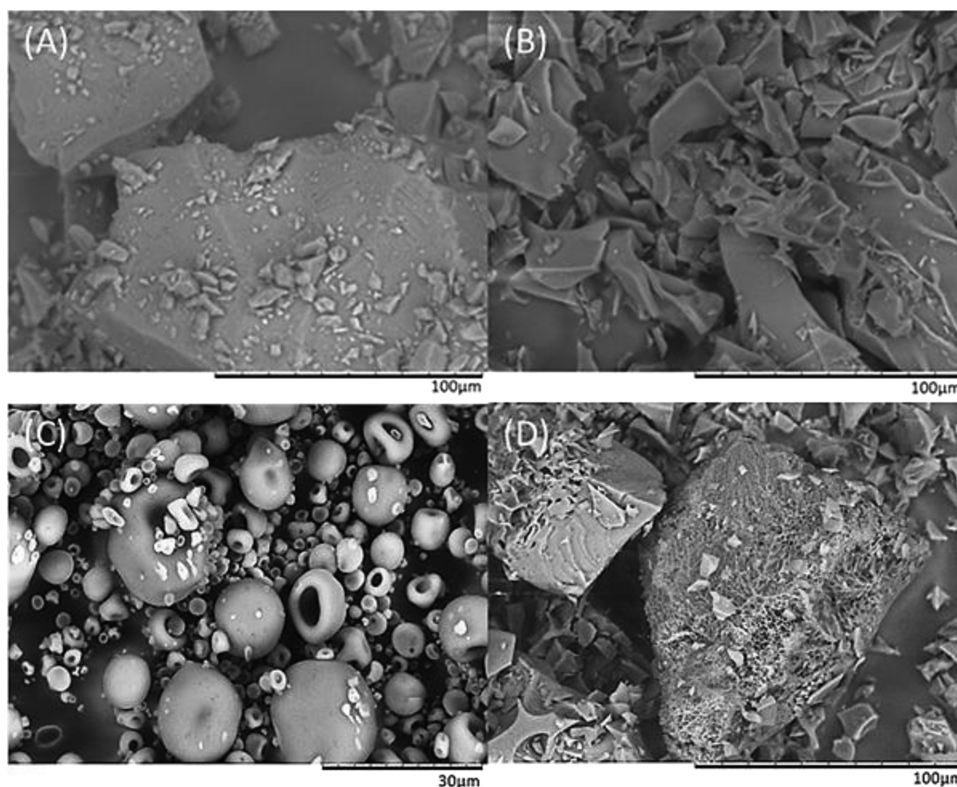
Figure 3. SEM image of the oven-dried LS particles (A), enzymatically polymerized oven-dried particles (B), spray-dried LS particles (C), and enzymatically polymerized spray-dried particles (D).

20% w/w), and the rate of change in the viscosity seen in the process can be described using a natural exponential-type equation, which is presented in Section 3.2 above. The regression of the model showed the fitting of the data, and an interpolation of 300 mPa s was also evaluated for the optimization, which is presented in Section 3.1.2 above. This empirical equation has previously been used to describe various cross-linking systems using Arrhenius-based systems showing curing of adhesives like epoxies, polyurethanes, and poly furfuryl alcohols.[23,24] The viscosity increase in the system due to polymerization was also seen in the case of fructose−amine−HMF systems, where the growing size of the polymer also affected the viscosity of the system along with temperature and flow conditions.[23]

The SEC data show the increase in the molecular weight increase at the rate of 414 Da/s in spray-drying as compared to only 328 Da/s in the case of oven-drying with higher molecular weights observed in the case of spray-drying due to which a proportional increase in viscosity was also observed with spray-drying having a higher viscosity in comparison to oven-drying by a difference of 1672 mPa s.

3.6. Phenolic Content. The drying temperature and the air velocity of drying contribute to the phenolic content of the material.[22] The LS showed a higher phenolic content in a bimodal distribution in the case of temperature (ranging between 5 and 6 mg/mL at the lowest (136.6 °C) to the highest (203.6 °C) temperature and 2.9 mg/mL at 170 °C) and with temperature at the center point, with the feeding rate and nozzle pressure playing a key role with the highest phenolic content of 6 mg/mL seen at low feeding rates and highest nozzle pressure, whereas a low phenolic content of 2.8 mg/mL seen at high feed rates and low nozzle pressures are

shown in Figure S3 of ESI. This shows that an optimum feeding rate and nozzle pressure are key to obtain particle atomization that can be used to preserve the phenolic content in the system.[22,25]

The inlet temperature of spray-drying has no effect on the particles as they are cooled instantly when the initial drying stage ends.[10,13] The outlet temperature of the system should be between 40 and 60 °C as it moves further in the drying chamber to preserve the highest amount of phenolics in the system. Similar results with regard to temperature were seen in the case of spray-drying of carbohydrates like maltodextrin and pekmez.[10,21]

3.7. Thermogravimetric Analysis. In this study, TGA was carried out to compare the thermal stability of the unpolymerized and polymerized spray-dried lignin, and the derivative TGA (DTG) curves can be seen in Figure 5. These show that the thermal stability of polymerized lignin is enhanced as compared to unpolymerized lignin. The final decomposition of the unpolymerized lignin happens at 775 °C,[26] whereas polymerized lignin had 13% mass remaining at the end of measurement at 900 °C. The initial degradation temperatures in both types of lignin are the same, but the decomposition is reduced in the case of polymerized LS, showing that longer chains and cross-linked networks keep the system more stable from thermal oxidation. The literature shows that in the case of polystyrene, cross-linking improves the thermal stability of the system in both argon and air atmosphere.[27] As the temperature goes up, the difference in the thermal oxidation is more and more prominent in pre- and postpolymerization processes. The changes in onsets and peaks in the DTG curve show that the number of cross-links and the uniformity of cross-linking control the degradation behavior of
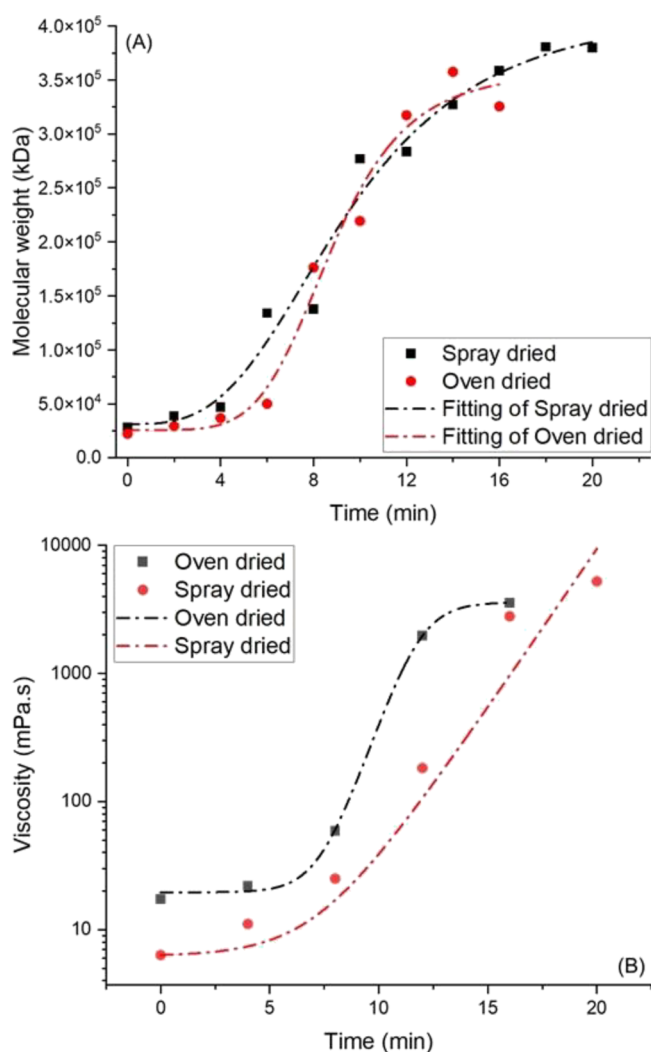
Figure 4. Molecular weight (A) and viscosity (B) increase evolution of the oven-dried and spray-dried LS.

the material.[27] The decomposition is not only less in the case of polymerized LS over the unpolymerized one, but all the peaks of decomposition have shifted. In the case of the unpolymerized lignin at the 200−300 °C range, the weaker aliphatic chains break from the aromatic structures.[28] Following which, above 400°, the formation of aromatic hydrocarbon phenolics and hydroxy phenolics dominate with the end stage of decomposition, where guaiacyl- and syringyl-type compounds are formed.[26,29] The last stage of the decomposition is the simultaneous formation and decomposition of lignin intermediates with the evolution of CO and C_1−C_3 hydrocarbons as mentioned after conducting GC/MS studies following a previous study.[30] For the polymerized lignin, these peaks were not observed at the abovementioned temperatures, which shows that not only the cross-linking made the material more thermostable in an oxidative environment but also opens opportunities for use of lignin in high-temperature applications and venture in to thermosets, plastics, and composites.[31]

3.8. Surface Charge and the Particle Size. The activity of the enzymes is strongly influenced by the properties of the material like size and surface charge, thus affecting sorption processes, conformation, and surface chemistry between the substrate and the enzymes.[32] Magnesium−LS are rich in the

sulfonyl group, which dissociate in water to form Mg^{2+} and Lignin coupled to the SO_3^- group that provides the negative charge to the material surface inside water.[33] During the zeta potential measurement, the spray-dried samples were measured both for the surface charge and the particle size. In terms of the particle size, spray-dried particles were 386 nm, whereas oven-dried particles had a particle size of 1.865 μm and for zeta potential, spray-dried lignin had a value of −26.5 mV, while oven-dried lignin had a value of −18.9 mV, which can be seen in Figure 6.

The significant difference in the particle size ratio of spray-dried LS to that of oven-dried (4.8 times) shows how the enzymes have an increased activity due to the changes in the spatial confinement, mobility, and curvature induced interactions.[20] The size of the particles along with surface chemistry such as hydrophilic interactions reduces the conformational changes in enzymes and also limits the structural changes and maintains the enzyme activity and integrity.[34] There are microenvironmental effects that can also be seen such as the catalytic efficiency of an enzyme is decreased with the increase in the particle size as there are mass transfer limitations that reduce the velocity at which the enzyme attaches to the surface of the substrate.[32,35] The increase in activity in the case of smaller particles is attributed to changes in the collision frequency between the enzyme and the substrate, as given by the Stokes−Einstein and collision theory equations.[36] These observations are also confirmed for lipase on gold nanoparticles and lactase dehydrogenase on varied sizes of glass pores.[32,34,35] Electrostatic groups present on the surface lead to the attraction and repulsion of the amino acids on the protein's surface or the entire enzyme. Laccases are also known as multicopper oxidases that contain three type of copper atoms based on unique spectroscopic features.[37] Type 1 and Type 2 copper centers each deliver electrons needed for conversion. The type 1 copper center contains two histidine and single cystine residues that are positively charged because of the presence of NH_2^+ groups, thus creating a hyperfine coupling with the lignin surface that is rich in the SO_3^- group.[33,38] Similar findings were observed in the case of higher activity of lactase bound to an anionic support as compared to a cationic support, proving that when an amino group is in contact with the surface, minimizing or maximizing these electrostatic interactions directly affects the distortion or precision of the enzyme adherence.[39]

4. CONCLUSIONS

Valorization of LSs continues to be of growing interest in scientific and commercial aspects in the range of applications relating to food, pharmaceutical, and consumer-based products. Despite the recent advancements in biorefineries, a robust downstream technique that not only preserves the substrate properties but also enhances the enzymatic interactions is the need of the chemoenzymatic syntheses. Through spray-drying, the amorphous structure of the LSs is retained with enhanced solubility. The effect of substrate modification by the minimization of the particle size to 385 nm from 1.865 μm, increase in surface charge from −18.9 to −26.5 mV, and a uniform surface topography were found in this research. It showed how the polymerization rate enhanced with molecular weight increase at a rate of 414 Da/s instead of 328 Da/s and a higher viscosity of 5232 mPa s. These values were observed after the optimization of the spray-drying process to have the maximum yield of dried mass at 65% and polymerization time
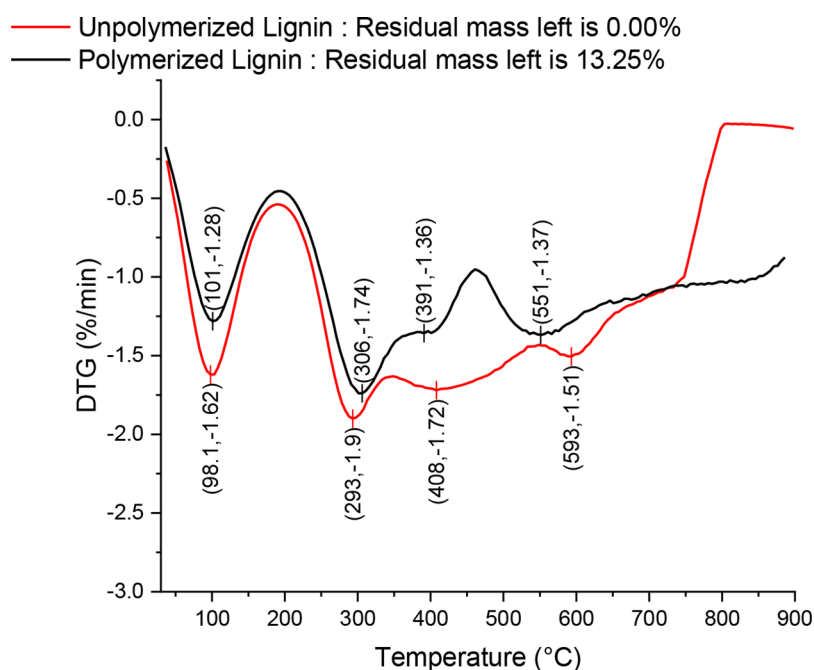
Figure 5. DTG curve of the enzymatically polymerized and unpolymerized spray-dried LS.
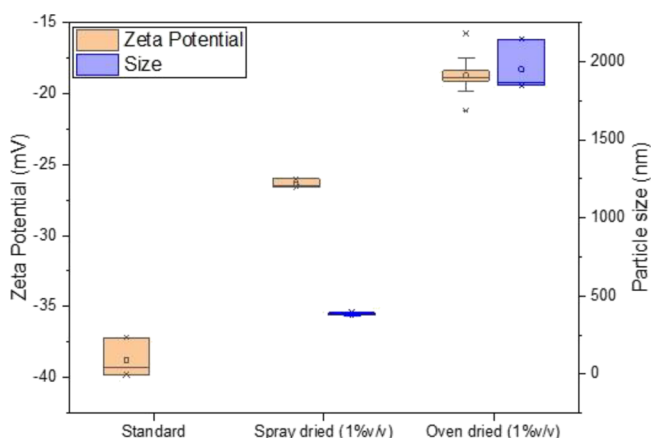

Figure 6. Zeta potential and particle size measurement of the oven-dried and spray-dried LS.

of 13 min at an inlet temperature of 190 °C, atomization at 45.6 mL/min, and a feeding rate of 12 mL/min.

AUTHOR CONTRIBUTION

S.S.P.P.: conceptualization, methodology, formal analysis, investigation, writing—original draft, and writing—review and editing. M.J.B.: formal analysis, investigation. A.P.: writing—review and editing, supervision. G.S.N.: writing—review and editing. H.W.G.v.H.: resources, writing—review and editing, supervision. G.M.G.: resources, writing—review and editing, supervision. N.S.: resources

ASSOCIATED CONTENT

Ⓢ Supporting Information

The Supporting Information is available free of charge at https://pubs.acs.org/doi/10.1021/acsomega.2c02421.

Table S1: Randomized DoE runs for drying and polymerization; Figure S1: Optimization of spray-drying of LS for enzymatic polymerization: Surface plot of the yield of the dried mass; Figure S2: Optimization of spray-drying of LS for enzymatic polymerization: Surface plot of the polymerization time. (PDF)

AUTHOR INFORMATION

Corresponding Author

Sidhant Satya Prakash Padhi − *Wood Kplus - Competence Center for Wood Composites & Wood Chemistry, Kompetenzzentrum Holz GmbH, Linz A-4040, Austria; Institute of Environmental Biotechnology, University of Natural Resources and Life Sciences, Vienna, Tulln an der Donau 3430, Austria;* ⓘ orcid.org/0000-0003-1713-7137; Email: s.padhi@wood-kplus.at, sidhant.padhi@boku.ac.at

Authors

Miguel Jimenez Bartolome − *Institute of Environmental Biotechnology, University of Natural Resources and Life Sciences, Vienna, Tulln an der Donau 3430, Austria;* ⓘ orcid.org/0000-0003-4143-5839

Gibson Stephen Nyanhongo − *Institute of Environmental Biotechnology, University of Natural Resources and Life Sciences, Vienna, Tulln an der Donau 3430, Austria; Department of Biotechnology and Food Technology, University of Johannesburg, Doornfontein 2028, South Africa;* ⓘ orcid.org/0000-0002-5379-8971

Nikolaus Schwaiger − *Sappi Papier Holding GmbH, Gratkorn 8101, Austria*

Alessandro Pellis − *Institute of Environmental Biotechnology, University of Natural Resources and Life Sciences, Vienna, Tulln an der Donau 3430, Austria; Dipartimento di Chimica e Chimica Industriale, Università degli Studi di Genova, Genova 16146, Italy;* ⓘ orcid.org/0000-0003-3711-3087

Hendrikus W. G. van Herwijnen − *Wood Kplus - Competence Center for Wood Composites & Wood Chemistry, Kompetenzzentrum Holz GmbH, Linz A-4040, Austria; Institute of Wood Technology and Renewable Materials, University of Natural Resources and Life Sciences, Vienna, Tulln an der Donau 3430, Austria*

Georg M. Guebitz − *Institute of Environmental Biotechnology, University of Natural Resources and Life Sciences, Vienna, Tulln an der Donau 3430, Austria*

Complete contact information is available at:
https://pubs.acs.org/10.1021/acsomega.2c02421

Notes

The authors declare no competing financial interest.

REFERENCES

(1) Aro, T.; Fatehi, P. Production and Application of Lignosulfonates and Sulfonated Lignin. *ChemSusChem* **2017**, *10*, 1861−1877.

(2) Van Heiningen, A. Converting a kraft pulp mill into an integrated forest biorefinery. *Pulp Paper Canada* **2006**, *107*, 38−43.

(3) Mattinen, M. L.; Suortti, T.; Gosselink, R. J. A.; Argyropoulos, D. S.; Evtuguin, D.; Suurnäkki, A.; Jong, E. D.; Tamminen, T. Polymerization of different lignins by laccase. *BioResources* **2008**, *3*, 549−565.

(4) Gil-Chávez, J.; Padhi, S. S. P.; Hartge, U.; Heinrich, S.; Smirnova, I. Optimization of the spray-drying process for developing aquasolv lignin particles using response surface methodology. *Adv. Powder Technol.* **2020**, *31*, 2348−2356.

(5) (a) Gil-Chávez, J.; Padhi, S. S. P.; Leopold, C. S.; Smirnova, I. Application of Aquasolv Lignin in ibuprofen-loaded pharmaceutical formulations obtained via direct compression and wet granulation. *Int. J. Biol. Macromol.* **2021**, *174*, 229−239. (b) Jimenez Bartolome, M.; Bischof, S.; Pellis, A.; Konnerth, J.; Wimmer, R.; Weber, H.; Schwaiger, N.; Guebitz, G. M.; Nyanhongo, G. S. Enzymatic synthesis and tailoring lignin properties: A systematic study on the effects of plasticizers. *Polymer* **2020**, *202*, No. 122725.

(6) Nyanhongo, G.; Gomes, J.; Gübitz, G.; Zvauya, R.; Read, J.; Steiner, W. Production of laccase by a newly isolated strain of Trametes modesta. *Bioresour. Technol.* **2002**, *84*, 259−263.

(7) Weiss, R.; Guebitz, G. M.; Pellis, A.; Nyanhongo, G. S. Harnessing the Power of Enzymes for Tailoring and Valorizing Lignin. *Trends Biotechnol.* **2020**, *38*, 1215−1231.

(8) (a) Tobimatsu, Y.; Schuetz, M. Lignin polymerization: how do plants manage the chemistry so well? *Curr. Opin. Biotechnol.* **2019**, *56*, 75−81. (b) Leonowicz, A.; Cho, N.; Luterek, J.; Wilkolazka, A.; Wojtas-Wasilewska, M.; Matuszewska, A.; Hofrichter, M.; Wesenberg, D.; Rogalski, J. Fungal laccase: properties and activity on lignin. *J. Basic Microbiol.* **2001**, *41*, 185−227.

(9) Shishir, M. R. I.; Chen, W. Trends of spray drying: A critical review on drying of fruit and vegetable juices. *Trends Food Sci. Technol.* **2017**, *65*, 49−67.

(10) Shofinita, D.; Langrish, T. A. G. Spray drying of orange peel extracts: Yield, total phenolic content, and economic evaluation. *J. Food Eng.* **2014**, *139*, 31−42.

(11) (a) Huber, D.; Pellis, A.; Daxbacher, A.; Nyanhongo, G. S.; Guebitz, G. M. Polymerization of Various Lignins via Immobilized Myceliophthora thermophila Laccase (MtL). *Polymer* **2016**, *8*, 280. (b) Huber, D.; Bleymaier, K.; Pellis, A.; Vielnascher, R.; Daxbacher, A.; Greimel, K. J.; Guebitz, G. M. Laccase catalyzed elimination of morphine from aqueous systems. *New Biotechnol.* **2018**, *42*, 19−25.

(12) Ortner, A.; Hofer, K.; Bauer, W.; Nyanhongo, G. S.; Guebitz, G. M. Laccase modified lignosulfonates as novel binder in pigment-based paper coating formulations. *React. Funct. Polym.* **2018**, *123*, 20−25.

(13) Blainski, A.; Lopes, G. C.; de Mello, J. Application and analysis of the folin ciocalteu method for the determination of the total phenolic content from Limonium brasiliense L. *Molecules* **2013**, *18*, 6852−6865.

(14) Behera, A.; Sahoo, S.; Patil, S. Enhancement of solubility: A pharmaceutical overview. *Der Pharm. Lett.* **2010**, *2*, 310−318.

(15) Saulick, Y.; Lourenço, S.; Baudet, B. Effect of particle size on the measurement of the apparent contact angle in sand of varying wettability under air-dried conditions. In *E3S Web of Conferences*; EDP Sciences, 2016: *9*, 09003.

(16) Littringer, E. M.; Mescher, A.; Schroettner, H.; Achelis, L.; Walzel, P.; Urbanetz, N. A. Spray dried mannitol carrier particles with tailored surface properties–the influence of carrier surface roughness and shape. *Eur. J. Pharm. Biopharm.* **2012**, *82*, 194−204.

(17) Maas, S. G.; Schaldach, G.; Walzel, P.; Urbanetz, N. A. Tailoring Dry Powder Inhaler Performance By Modifying Carrier Surface Topography By Spray Drying. *Atomiz. Spr.* **2010**, *20*, 763−774.

(18) Matsuno, H.; Nagasaka, Y.; Kurita, K.; Serizawa, T. Superior activities of enzymes physically immobilized on structurally regular poly (methyl methacrylate) surfaces. *Chem. Mater.* **2007**, *19*, 2174−2179.

(19) Roach, P.; Farrar, D.; Perry, C. C. Surface tailoring for controlled protein adsorption: effect of topography at the nanometer scale and chemistry. *J. Am. Chem. Soc.* **2006**, *128*, 3939−3945.

(20) Shang, W.; Nuffer, J. H.; Dordick, J. S.; Siegel, R. W. Unfolding of ribonuclease A on silica nanoparticle surfaces. *Nano Lett.* **2007**, *7*, 1991−1995.

(21) Akkaya, Z.; Schröder, J.; Tavman, S.; Kumcuoglu, S.; Schuchmann, H. P.; Gaukel, V. Effects of Spray Drying On Physical Properties, Total Phenolic Content And Antioxidant Activity Of Carob Molasses. *Int. J. Food Eng.* **2012**, *8*, 20.

(22) Zhang, J.; Zhang, C.; Chen, X.; Quek, S. Y. Effect of spray drying on phenolic compounds of cranberry juice and their stability during storage. *J. Food Eng.* **2020**, *269*, No. 109744.

(23) Thoma, C.; Solt-Rindler, P.; Sailer-Kronlachner, W.; Rosenau, T.; Potthast, A.; Konnerth, J.; Pellis, A.; van Herwijnen, H. W. G. Carbohydrate-hydroxymethylfurfural-amine adhesives: Chemorheological analysis and rheokinetic study. *Polymer* **2021**, *231*, No. 124128.

(24) (a) Mohajeri, S.; Vafayan, M.; Ghanbaralizadeh, R.; Pazokifard, S.; Zohuriaan Mehr, M. J. Advanced isoconversional cure kinetic analysis of epoxy/poly(furfuryl alcohol) bio-resin system. *J. Appl. Polym. Sci.* **2017**, *134*, 45432. (b) Cañamero-Martínez, P.; Fernández-García, M.; de la Fuente, J. L. Rheological cure characterization of a polyfunctional epoxy acrylic resin. *React. Funct. Polym.* **2010**, *70*, 761−766.

(25) (a) Mishra, P.; Mishra, S.; Mahanta, C. L. Effect of maltodextrin concentration and inlet temperature during spray drying on physicochemical and antioxidant properties of amla (Emblica officinalis) juice powder. *Food Bioprod. Process.* **2014**, *92*, 252−258. (b) Caliskan, G.; Nur Dirim, S. The effects of the different drying conditions and the amounts of maltodextrin addition during spray drying of sumac extract. *Food Bioprod. Process.* **2013**, *91*, 539−548.

(26) Brebu, M.; Vasile, C. Thermal degradation of lignin—a review. *Cellul. Chem. Technol.* **2010**, *44*, 353−363.

(27) Levchik, G. F.; Si, K.; Levchik, S. V.; Camino, G.; Wilkie, C. A. The correlation between cross-linking and thermal stability: Cross-linked polystyrenes and polymethacrylates. *Polym. Degrad. Stab.* **1999**, *65*, 395−403.

(28) Murwanashyaka, J. N.; Pakdel, H.; Roy, C. Step-wise and one-step vacuum pyrolysis of birch-derived biomass to monitor the evolution of phenols. *J. Anal. Appl. Pyrolysis* **2001**, *60*, 219−231.

(29) (a) Rodrigues, J.; Graça, J.; Pereira, H. Influence of tree eccentric growth on syringyl/guaiacyl ratio in Eucalyptus globulus wood lignin assessed by analytical pyrolysis. *J. Anal. Appl. Pyrolysis* **2001**, *58-59*, 481−489. (b) Alén, R.; Kuoppala, E.; Oesch, P. Formation of the main degradation compound groups from wood and its components during pyrolysis. *J. Anal. Appl. Pyrolysis* **1996**, *36*, 137−148.

(30) Boateng, A. A.; Hicks, K. B.; Vogel, K. P. Pyrolysis of switchgrass (Panicum virgatum) harvested at several stages of maturity. *J. Anal. Appl. Pyrolysis* **2006**, *75*, 55−64.

(31) Chen, Y.; Stark, N. M.; Cai, Z.; Frihart, C. R.; Lorenz, L. F.; Ibach, R. E. Chemical modification of kraft lignin: effect on chemical and thermal properties. *BioResources* **2014**, *9*, 5488−5500.

(32) Talbert, J. N.; Goddard, J. M. Enzymes on material surfaces. *Colloids Surf. B Biointerfaces* **2012**, *93*, 8−19.

(33) Luxbacher, T. *The ZETA guide: Principles of the streaming potential technique*. Anton Paar GmbH: Graz, Austria 2014.

(34) El-Zahab, B.; Jia, H.; Wang, P. Enabling multienzyme biocatalysis using nanoporous materials. *Biotechnol. Bioeng.* **2004**, *87*, 178−183.

(35) Wu, C. W.; Lee, J. G.; Lee, W. C. Protein and enzyme immobilization on non-porous microspheres of polystyrene. *Biotechnol. Appl. Biochem.* **1998**, *27*, 225−230.

(36) Wu, C.-S.; Lee, C.-C.; Wu, C.-T.; Yang, Y.-S.; Ko, F.-H. Size-modulated catalytic activity of enzyme−nanoparticle conjugates: a combined kinetic and theoretical study. *Chem. Commun.* **2011**, *47*, 7446−7448.

(37) Jones, S. M.; Solomon, E. I. Electron transfer and reaction mechanism of laccases. *Cell. Mol. Life Sci.* **2015**, *72*, 869−883.

(38) Solomon, E. I.; Sundaram, U. M.; Machonkin, T. E. Multicopper oxidases and oxygenases. *Chem. Rev.* **1996**, *96*, 2563−2606.

(39) (a) Haupt, B.; Neumann, T.; Wittemann, A.; Ballauff, M. Activity of enzymes immobilized in colloidal spherical polyelectrolyte brushes. *Biomacromolecules* **2005**, *6*, 948−955. (b) Lund, M.; Åkesson, T.; Jönsson, B. Enhanced protein adsorption due to charge regulation. *Langmuir* **2005**, *21*, 8385−8388. (c) Hamlin, R. E.; Dayton, T. L.; Johnson, L. E.; Johal, M. S. A QCM study of the immobilization of β-galactosidase on polyelectrolyte surfaces: Effect of the terminal polyion on enzymatic surface activity. *Langmuir* **2007**, *23*, 4432−4437.